

## SEISMIC CONTROL OF CABLE-STAYED BRIDGES USING SHAPE MEMORY ALLOY DAMPERS

A. Sharabash<sup>1</sup> and B. Andrawes<sup>2</sup>

<sup>1</sup> Postdoctoral Scholar, Dept. of Civil and Environmental Engineering, University of Illinois at Urbana-Champaign, USA

<sup>2</sup> Assistant Professor, Dept. of Civil and Environmental Engineering, University of Illinois at Urbana-Champaign, USA

Email: [alaa@uiuc.edu](mailto:alaa@uiuc.edu), [andrawes@uiuc.edu](mailto:andrawes@uiuc.edu)

### ABSTRACT :

The superelasticity and damping capability of the shape memory alloys (SMAs) are sought in this study to develop a supplementary recentering and energy dissipation device for cable-stayed bridges. This paper introduces and investigates the performance of a new passive seismic control device for cable-stayed bridges made with SMAs. A three-dimensional long-span bridge model including the effect of soil-structure interaction is developed and utilized in the study. SMA dampers are implemented at the bridge's deck-pier and deck-tower connections. The bridge is subjected to three orthogonal components from a historic ground motion record. The effectiveness of the SMA dampers in controlling the deck displacement and limiting the shear and bending moment demands on the bridge towers is assessed. The analytical results show that SMA dampers can successfully control the seismic behavior of the bridge. However, the effectiveness of the new dampers is significantly influenced by the relative stiffness between the dampers used at the deck-tower and deck-pier connections.

**KEYWORDS:** Cable-stayed bridges, Shape memory alloys, Seismic, Dampers

### 1. INTRODUCTION

Cable-stayed bridges are flexible extended-in-plane structures which provide an aesthetic and practical solution for long spans. The extreme flexibility of the structure has concerned many researchers and engineers especially under extreme dynamic loads such as earthquakes. Studies have proven that although restraining the bridge deck completely at the pier and tower locations could limit the deck displacement, it would cause a significant increase in the demands on the piers and towers in terms of bending moment and shear forces (Ali and Abdel-Ghaffar 1994). Therefore, there is an agreement among many researchers that the main deck should neither be fixed to the towers nor to the piers, but rather be allowed to experience some sort of relative movement at these locations, which would lead to a reduction in the overall forces transmitted between the superstructure and the substructure. In order for this solution to be implemented successfully and since cable-stayed bridges possess little damping characteristics that may not always be enough to help alleviate vibration under severe ground motions, supplementary damping devices is often sought. This fact introduces new challenges to the earthquake engineering community in terms of seeking and developing new damping technologies that could improve the seismic performance of cable-stayed bridges.

In recent years, considerable attention has been paid to research and development of structural control devices, with particular emphasis on dynamic control devices for cable-stayed bridges. These devices are typically divided into passive, semi-active, and active control devices (Soong and Dargush 2003). This study presents a new class of dampers that could overcome many of the shortcomings of other dampers such as plastic deformation and lack of recentering. The new damper is made of superelastic Shape Memory Alloys (SMAs); a relatively new class of metallic alloys which exhibit unique mechanical characteristics. The number of studies focusing on the feasibility

of using SMAs in seismic applications has grown in the past decade and is still growing [Yan and Nei 2003 & Hui et al. 2004]. The work presented in this paper is primarily directed towards the potential application of SMAs as seismic passive damper devices for vibration mitigation of cable-stayed bridges.

## 2. CABLE-STAYED BRIDGE

### 2.1. Bridge Description

Three-dimensional hypothetical bridge model, suggested by Abdel-Ghaffar and Nazmy (1991) was adopted in this study. Figure 1 shows a schematic elevation of the bridge and its A-shaped towers. As shown in the figure, the bridge has a center span of 670.5m and side spans of 292.6m. The two A-shaped central towers supporting the bridge had a height of 170.8m and a width at the foundation level equal to 36.0m. The end spans of the bridge were supported by two piers.

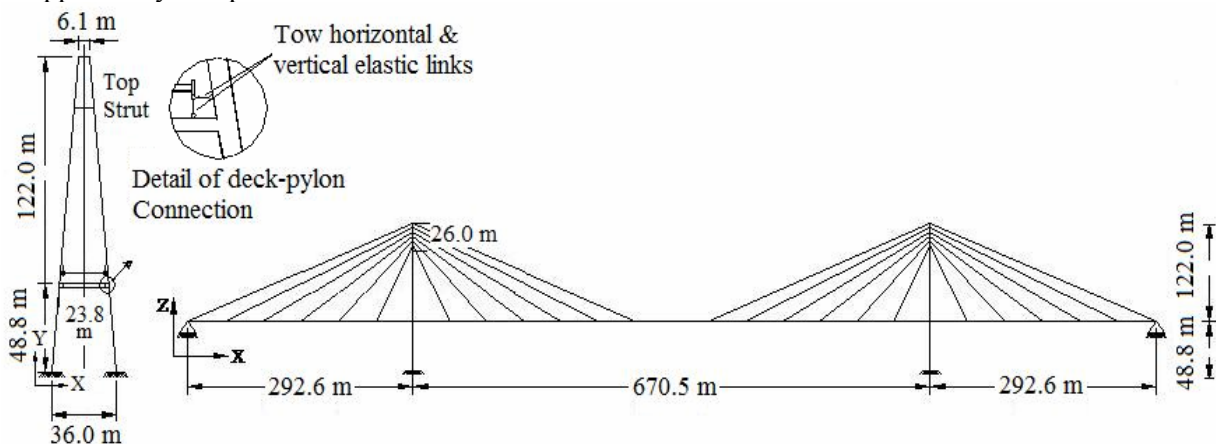


Figure 1 Schematic of cable-stayed bridge adopted in the study

Shock-transmission devices were assumed at the deck-tower connection to limit the displacement of the deck. These devices allow the movement of the deck due to temperature changes, but rigidly connect the tower and deck together under a strong motion. On the other hand, bearings at both piers of the reference bridge were modeled such that they would permit movement in the longitudinal direction and rotation about the transverse and vertical axes i.e. the Y-axis and Z-axis, respectively. These boundary conditions are identical to the boundary conditions of the benchmark problem bridge that was suggested by the ASCE Committee on Structural Control (Dyke et al. 2000). The committee recommended using these boundary conditions as a basis for the comparison with various structural control devices.

### 2.2. Analytical Model of Reference Bridge

The 3-D finite element model of the reference bridge (i.e. bridge with no SMA dampers) that was used as the basis for the comparison in this study is depicted in Fig. 2. The model was developed and analyzed using the open-source finite element program OpenSees (Mazzoni et al. 2006). The models of the bridge deck and towers were developed using 94 nodes, 121 elastic beam-column elements and 48 truss elements. In the original bridge model presented by Abdel-Ghaffar and Nazmy (1991), the effect of soil-structure interaction (SSI) was neglected. However, in this study the SSI was considered and modeled using a series of translational and rotational springs and dashpots introduced at the base of the bridge towers in the three global directions X, Y and Z (see Fig. 2). In order to provide a realistic representation of the SSI in the studied bridge, the central towers were assumed to be connected at the base to two embedded gravity-type deep open concrete caisson foundations. The base dimensions of each foundation block were assumed to be equal to 50mx40m, with a depth of 30m. Subsoil supporting the foundation was assumed to be soft saturated clay with soil modulus of elasticity  $E_s$  of 15MPa,

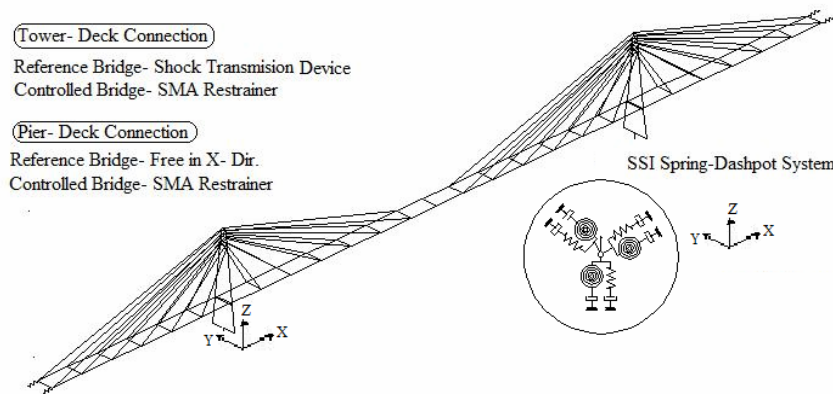


Figure 2  
 Three-dimensional finite element idealization of the cable-stayed bridge adopted in the study

Poisson ratio  $\nu$  of 0.45, and shear wave velocity  $V_s$  of 150m/s. Using Eqn. 2.1, the shear modulus of elasticity  $G_s$  is found to be 5.17MPa.

$$G_s = E_s / (2(1 + \nu)) \quad (2.1)$$

In this study, the simplified equivalent modal energy method presented by Novak (1974) was utilized to describe the effect of SSI. In this method, the soil is replaced by a spring-dashpot system, where damping and stiffness coefficients are obtained from the results of the half space analysis of rigid circular footing as given by Veletsos and Wei (1971); Veletsos and Verbic (1973) where the subsoil is assumed to behave elastically with no energy dissipation and the foundation is idealized as a rigid, massless circular plate. OpenSees was utilized in performing the modal analysis of the bridge assuming a damping factor of 2%. The first three natural periods of the model were 5.53, 4.23 and 4.15sec.

### 3. GROUND MOTION

In order to conduct a close and precise evaluation of the analyzed bridge with the SMA dampers the bridge was subjected to the three orthogonal components of a single record from the 1995 Kobe earthquake in Japan. Although the results are based only on one record, they can explain the nature of the problem and indicate the sensitivity of the response to the SMA devices. The record was obtained from station 0 at Nishi-Akashi which is located at a distance of 11.1kms from the epicenter of the earthquake. The three orthogonal components NIS000, NIS090 and NIS-up were applied in the longitudinal, lateral and vertical directions of the bridge, respectively. Figure 3 shows the ground acceleration time history of the three components. As shown in the figure, the maximum ground acceleration of the NIS000, NIS090, and NIS-UP record components were 0.509g, 0.503g, and 0.371g, respectively.

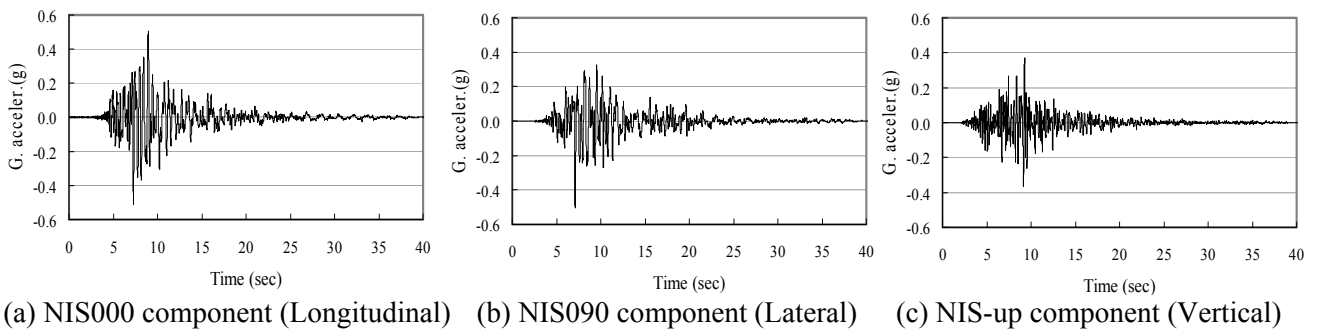


Figure 3 Ground motion time history of the three components of the Nishi-Akashi record from the 1995 Kobe, Japan earthquake

## 4. SHAPE MEMORY ALLOYS

### 4.1 Background and Model Description

SMA form a relatively new class of metallic alloys that possess unique capability to restore their original shape after being deformed excessively to a strain that could reach up to 8%. The key behind such unique feature lies in the ability of the SMA to transform from the austenite phase to the martensite phase and vice versa. Phase transformation is triggered by mechanical or thermal loading. Based on the manufacturing process and chemical composition, a SMA could be categorized as either superelastic (i.e. recover its original shape when unloaded) or shape memory (i.e. recovers its original shape when heated). This study will focus on the former SMA type. Figure 4a shows a schematic of the stress-strain relation typically observed in superelastic SMAs. As shown in the figure, the stress-strain behavior of superelastic SMAs could be divided into three phases: (1) linear austenite, (2) phase transformation, and (3) linear martensite. The phase transformation is characterized by a very low modulus and thus resembles yielding in materials with typical plastic behavior. When the applied stress is removed the martensite becomes unstable and thus converts back to austenite resulting in the shown “flag shape” hysteresis. As shown in the figure, superelastic SMAs possess several characteristics that make them ideal for seismic applications including hysteretic damping, recentering capability (i.e. ability of the material to return to its undeformed configuration upon unloading), ability to undergo strain hardening at large strain levels (>6%-strain), and the formation of stress plateau during phase transformation which controls the forces transmitted to the structure.

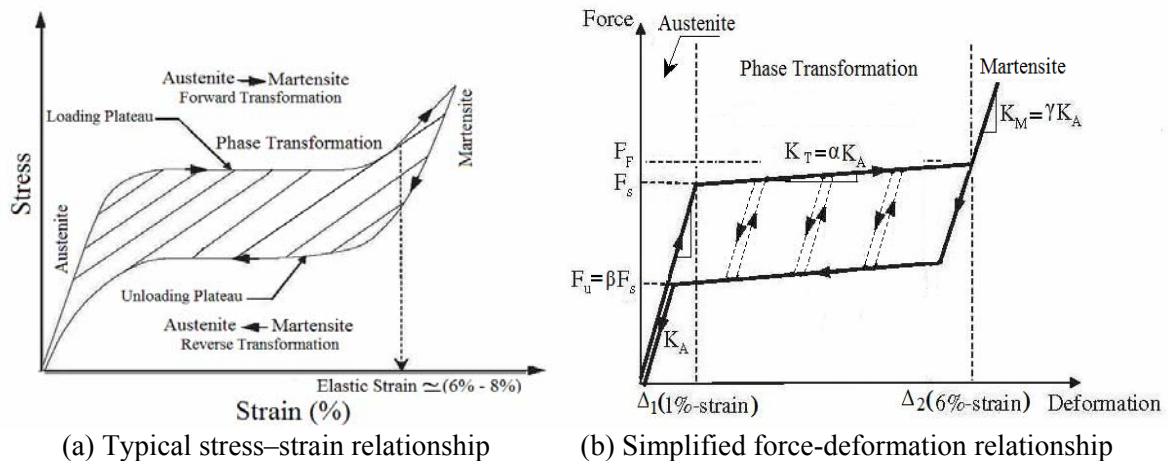


Figure 4 Typical stress-strain and simplified force-deformation relationships of superelastic SMAs

In order to describe the constitutive behavior of the SMAs realistically, a one-dimensional tension-only SMA material model was developed and implemented in the OpenSees material library and used in the study. This model is capable of describing the force-deformation relationship of superelastic SMAs at a constant temperature (i.e. the model is temperature independent). A schematic of the force-deformation relation of the SMA model adopted in this study is presented in Fig. 4b. The model was defined by six parameters. Those parameters are austenite elastic stiffness  $K_A$ , transformation elastic stiffness  $K_T$  ( $\alpha K_A$ ), martensite elastic stiffness  $K_M$  ( $\gamma K_A$ ), phase transformation starting force  $F_S$ , phase transformation finishing force  $F_F$ , and the unloading force at the end of the reverse transformation  $F_U$  ( $\beta F_S$ ). The SMA model represents an idealized behavior for the SMA devices where a complete recovery of the original shape is achieved at the end of each cycle. In this model, the strain at the start and the end of the phase transformation were fixed and were taken equal to 1% and 6%, respectively. These values are typical for superelastic SMAs (Otsuka and Wayman 2002).

#### 4.2 Design of SMA Device

The SMA damping device considered in this study was in the form of cables consisting of bundled or twisted SMA wires and connecting the deck with the piers and towers. The size and number of these cables can vary depending on the level of force and stiffness desired. However, in order to minimize the number of variables, the length of the SMA cables was assumed to be constant regardless of the location where the cables were used. As an alternative for using a tension-compression device, two tension-only SMA elements were connected to both sides of the deck relative to the pier and tower. These elements were superimposed where one element is engaged when the structural displacement is positive, whereas the other element starts engaging when the displacement is negative. The two elements were assumed to be identical in their mechanical properties and act symmetrically under reversible loading. Figure 5 shows schematic of the configuration proposed for SMA damper cable for the pier-deck and tower-deck connections.

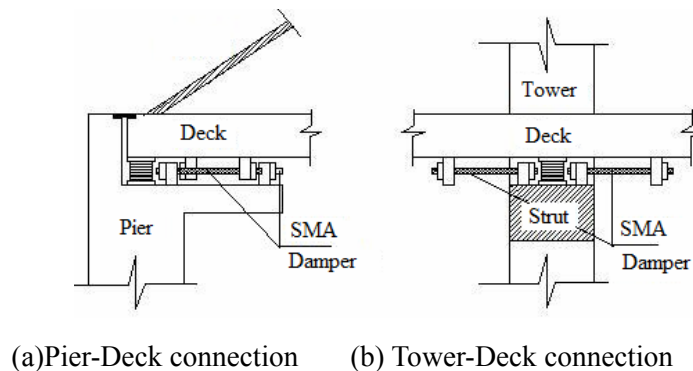


Figure 5 Schematic of the configuration proposed for SMA dampers at pier and tower connections.

The design of the SMA devices was related directly to the response of the reference bridge through defining a reference force  $F_R$  and reference displacement  $\Delta_R$  from the reference bridge response and utilizing these values in determining the mechanical characteristics of SMA devices. The reference force in this study was defined as the maximum reaction force exerted by the shock transmission devices connecting the towers and the deck, while the reference displacement was taken as the maximum displacement of the deck at the pier location. Since the length of the SMA cables was assumed to be constant, the amount of cable deformation at the end of the phase transformation (i.e. at 6%-strain) was taken as constant. The relative displacement between the two ends of the SMA cables at the end of phase transformation was limited to  $\Delta_R/2$ . This would allow the SMA device to experience at least 50% of its phase transformation which is a key factor in defining the level of hysteretic damping introduced to the structure by the SMAs without transferring excessively large level of forces to the deck. On the other hand, the level of force introduced to the system by the SMA device which would define the number of SMA cables used at each location was defined as a ratio of  $F_R$ .

## 5. SENSITIVITY STUDY

### 5.1 Description of the Sensitivity Study

The effectiveness of the SMA device in controlling the dynamic response of the bridge was evaluated through a sensitivity study. The primary aim of the study was to assess the level of response improvement using SMA devices with various stiffness and phase transformation forces. Another important aspect of the study was to determine the optimum distribution ratio of SMA devices between the tower and pier connections. The SMA's phase transformation force  $F_S$  was computed as  $F_S = (k_{S/R}) \cdot F_R$ , where  $k_{S/R}$  is a factor that could take a value between 0.0 and 1.0, and  $F_R$  is the reference force described earlier. The factor  $k_{S/R}$  specifies the level of force desired in the bridge connection where the SMA device is installed and accordingly determine the number of SMA cables required to reach this level of force. The force  $F_S$  was then distributed between the SMA dampers at the tower and pier locations using the distribution factor  $K_{P/S} = F_P/F_S$  which can take values between 0.0 and 1.0,

where  $F_p$  is the force assigned to the SMA dampers at the pier location. The value 0.0 indicates that the SMA dampers are used entirely at the deck-tower connections and that the deck is free at the piers location, while the value 1.0 indicates that the SMA dampers are used entirely at the deck-pier connections and the deck is totally floating at the tower locations. The factors  $k_{S/R}$  and  $k_{P/S}$  and the reference displacement  $\Delta_R$  were used to compute the stiffness of SMA dampers used at each location. The strain hardening ratios of the SMAs during phase transformation ( $\alpha$ ) and martensitic phase ( $\gamma$ ) (see Fig. 4b) were assumed to be constant and equal to 0.05 and 1.0, respectively. Furthermore, parameter  $\beta$  which defines the ratio between the unloading and loading stresses at the end and start of phase transformation, respectively was also assumed to be constant and equal to 0.4. The sensitivity study was conducted considering the two parameters  $k_{S/R}$  and  $k_{P/S}$  as variables while the response parameters which were monitored as the primary outcome of the study was: (1) maximum displacement of the deck in the longitudinal direction (X-direction)  $D$ , (2) maximum shear force at the base of the two towers in the longitudinal direction  $V$ , and (3) maximum bending moment at the base of the two towers about the lateral axis (Y-axis)  $M$ . The response parameters were presented in a normalized format relative to the reference bridge responses.

### 5.2 Results of the Sensitivity Study

A summary of the results obtained from the sensitivity study is presented in Figure 6. Figures 6.a, 6.b, and 6.c show the variation of the normalized maximum deck displacement, maximum base shear at the towers, and maximum base moments at the towers, respectively with the two parameters  $k_{P/S}$  and  $k_{S/R}$ . The three figures show a significant improvement in the overall response of the SMA-controlled bridge compared to the reference bridge. The SMA dampers were able to reduce the maximum bridge displacement, towers base shear, and towers base moment by up to 67%, 71%, and 70%, respectively compared to the responses of the reference bridge. It is also clear from the figures that the case where  $k_{S/R}$  is equal to 0.4 which would result in the least amount of SMA force and thus the least number of SMA dampers results in an extremely less effective performance compared to other cases. A slight increase in the number of dampers which could be represented by the case of  $k_{S/R}=0.5$  would result in a significant improvement in the overall bridge performance compared to the case of  $k_{S/R}=0.4$  (e.g. 45% reduction in maximum displacement). Increasing the number of SMA dampers further would improve the overall bridge performance with an extent that depends on the distribution of the dampers between pier and tower connections, i.e. depending on the value of  $k_{P/S}$ . Minor differences in the bridge response is observed at higher values of  $k_{P/S}$ , which indicates that a more efficient design of these dampers in terms of reducing the number of dampers could be achieved by providing more concentration of the dampers at the pier location rather than the tower location. Furthermore, the three figures show similar trends in terms of observing nonlinear reduction in the bridge responses with the increase in the ratio of SMA dampers at the piers relative to the towers, i.e. larger values of  $k_{P/S}$ . This observation is true regardless of the  $k_{S/R}$  value. However, the responses reach an almost stable condition at a factor  $k_{P/S}$  close to 0.5 which represents providing 50% of the SMA dampers at each of the pier and tower connections. This is especially true for the case with moderate to high  $k_{S/R}$  ratio (i.e.  $k_{S/R}>0.5$ ). However, for the case where  $k_{S/R}$  is equal to 0.5, a stable response is observed at a  $k_{P/S}$  value of 0.75.

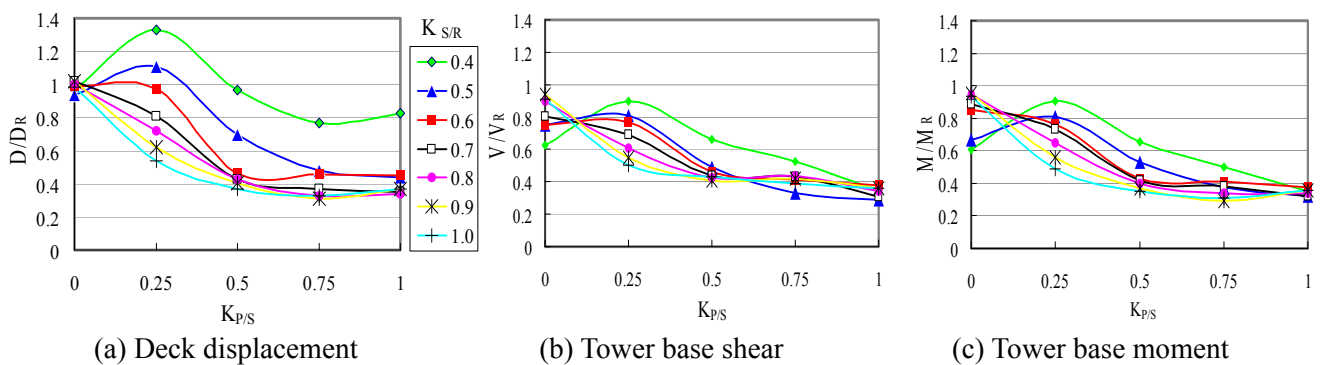


Figure 6. Normalized maximum bridge responses with various  $K_{S/R}$  and  $K_{P/S}$  values.

## 6. CASE STUDY

A case study aiming at providing a better understanding of the behavior of the SMA dampers was conducted. The results presented in Fig. 6 showed that the most economic though still effective case was when  $k_{S/R}$  was taken as 0.5. Providing more SMA dampers would not affect the controlled bridge response dramatically, especially when most of the dampers are located at the pier connection. Therefore, in this case study the  $k_{S/R}$  and  $k_{P/S}$  ratios were assumed to be 0.5 and 0.75, respectively. Figures 7a, 7b, and 7c show a comparison between the time histories of the deck displacement, tower base shear, and tower base moment responses, respectively for the SMA-controlled bridge and the reference bridge under the three components of the Nishi-Akashi record from the 1995 Kobe earthquake. The figures show that the SMA dampers were able to reduce the maximum responses of the bridge significantly. The maximum deck displacement of the reference bridge was 200mm and was reduced by using the SMA dampers by approximately 54% to a displacement value of 93mm. Similarly, the maximum tower base shear was reduced to 10.29MN with SMAs compared to 30.59MN without SMAs, which represents a reduction of 66%. The maximum tower base moment was also reduced to 447.37MN.m compared to 1237.34MN.m, which represents a reduction of 64%. In order to provide information on the mechanical behavior of the SMA dampers, the force-displacement relation of the SMA dampers used at the pier and tower connections are presented in Figures 8a and 8b, respectively. As shown in the figures the total force in the SMA dampers used at the piers was approximately three times the force in the dampers used at the tower connections. This was due to the fact that 75% of the total SMA dampers were allocated at the pier connections while the remaining 25% were allocated at the towers connection. The maximum force observed in the SMA dampers at the pier connections was approximately 6.58MN, while for the tower connections the maximum force reached by the dampers was 2.03MN. In this particular case the total reaction force resulted from using shock transmission devices at the tower connection of the reference bridge was 14.43MN. This shows that the SMAs plateau was successful in limiting the level of force in the connections effectively.

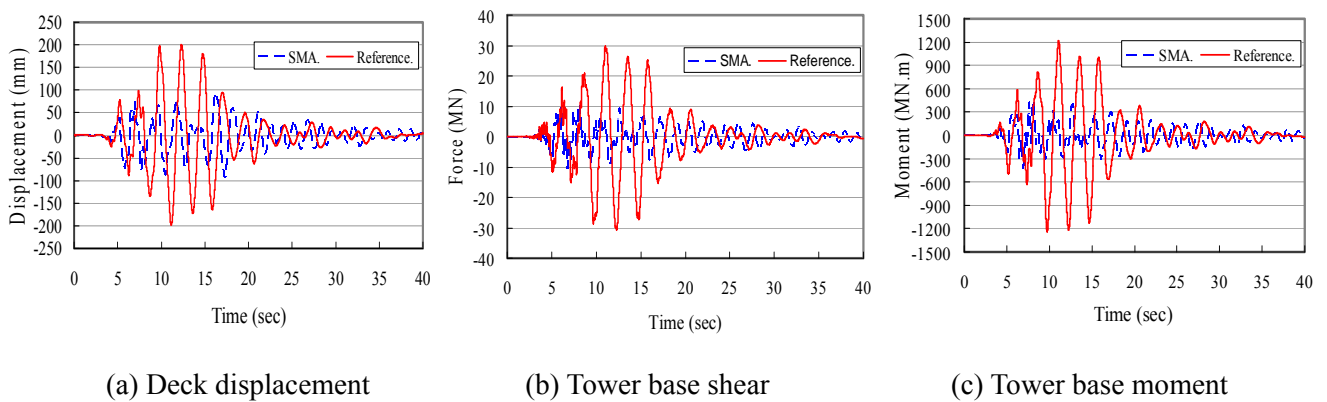


Figure 7 Response time histories of the SMA controlled cable-stayed bridge compared to the reference bridge.

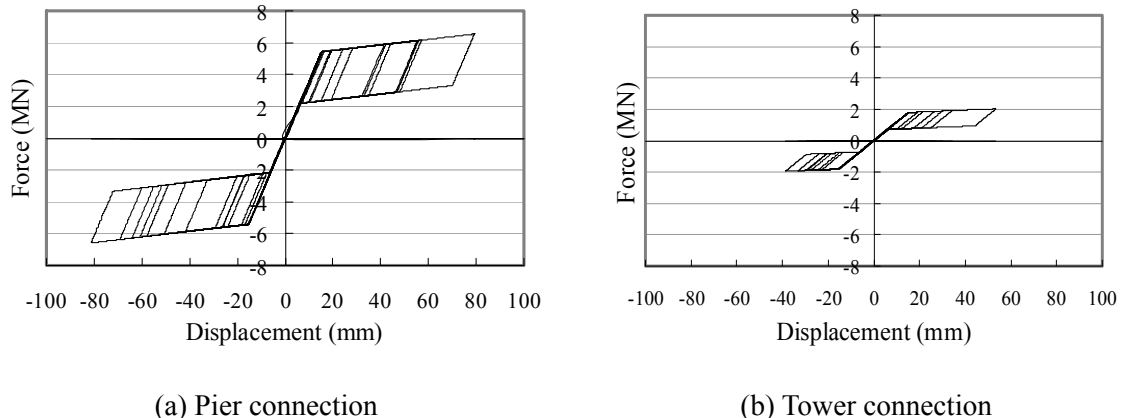


Figure 8. Force-displacement responses of the SMA dampers used at the pier and tower connections

## 7. CONCLUSIONS

This analytical paper focused on evaluating the effectiveness of using superelastic SMA dampers for the seismic control of cable-stayed bridges. A 3-D cable-stayed bridge model including the effect of soil-structure interaction was developed and utilized in the study. SMA dampers were implemented at the deck-pier and deck-tower connections. The bridge was subjected to the three orthogonal components of the Nishi-Akashi record from the 1995 Kobe earthquake in Japan. The seismic behavior of the SMA-controlled bridge was compared with the behavior of a reference bridge with shock-transmission devices at the deck-tower connections. The design of the SMA dampers was directly related to the response of the reference bridge. A sensitivity study was conducted to assess the effect of variability of the stiffness and phase transformation force of the SMA dampers on their effectiveness. The results of the study show that SMA dampers were able to reduce the maximum bridge displacement, towers base shear, and towers base moment by up to 67%, 71%, and 70%, respectively compared to the responses of the reference bridge. It was also found that increasing the number of SMA dampers would improve the overall bridge performance with an extent that depends on the distribution of the dampers between pier and tower connections. However, the most efficient design of SMA dampers was observed when the summation of the phase transformation forces of the dampers used at the tower and pier connections was 50% of the force in the reference bridge at the tower connection. The most efficient distribution for the dampers between the pier and tower connections was observed when 50%-75% of the dampers were allocated at the pier connections.

## REFERENCES

- Abdel-Ghaffar, A.M., and Nazmy, A.S. (1991). 3-D Non-Linear Seismic Behaviour of Cable-Stayed Bridges. *ASCE, Journal of Structural Engineering* 117:11, 3456-3476.
- Ali, H.M., and Abdel-Ghaffar, A.M. (1994). Seismic energy dissipation for cable-stayed bridges using passive devices. *Earthquake Engineering and Structural Dynamics* 23, 877-893.
- Dyke, J., Caicedo J., Turan, G., Bergman, L. and Hague D. (2000). Benchmark Control Problem for Seismic Response of Cable-stayed Bridge. <http://wusceel.cive.wustl.edu/quake/benchmark/>
- Mazzoni, S., McKenna, F., Scott M., Fenves, G., et al. (2006). Open System for Earthquake Engineering Simulation. OpenSees Command Language Manual. Pacific Earthquake Engineering Research Center, University of California, Berkeley.
- Novak, M. (1974). Effect of Soil on Structural Response to Wind and Earthquake. *Earthquake Engineering and Structural Dynamics* 3, 79-86.
- Otsuka, K. and Wayman, C. (2002). Shape memory materials, Cambridge University Press.
- Soong, T. and Dargush, G. (1997). Passive energy dissipation systems in structural engineering, Wiley, London.
- Veletsos, A., and Verbic B. (1973). Vibration of viscoelastic foundations. *J. Earthquake Engrg. Struct. Dyn.* 2:1, 87-102.
- Veletsos, A., and Wei, Y. (1971). Lateral and rocking vibrations of footings. *J. Soil Mech. and Found. Div., ASCE* 97:9, 1227-1248.
- Yan, XJ., and Nie, JX. (2003). Study of a new application form of shape memory alloy superelasticity. *Smart Materials and Structures* 12,N14-N23.